Bulgarian Chemical Communications, Volume 50, Special issue H (pp. 189–195) 2018

DRIFT study of the mechanism of methanol synthesis from CO_2 and H_2 on CeO_2-supported CaPdZn catalyst

A. S. Malik, S. F. Zaman*, A. A. Al-Zahrani, M. A. Daous, H. Driss, L. A. Petrov

Chemical and Materials Engineering Department, Faculty of Engineering, King Abdulaziz University, P.O. Box 80204, Jeddah 21589, Saudi Arabia

Received: February 02, 2018; Revised, March 23, 2018

This article reports results of mechanistic DRIFTS study of methanol synthesis from CO_2 and H_2 on CaPdZn/CeO_2 catalyst. The catalyst exhibited superior catalytic performance with ~100% selectivity to methanol and 7.7% conversion of CO_2 at 30 bar and 220 °C. In situ DRIFTS measurements were carried out under experimental conditions and the presence of various surface reaction intermediate species and their subsequent conversion to methanol were carefully monitored. The catalyst was characterised by BET, CO chemisorption, CO_2-TPD, and HRTEM to evaluate the physiochemical properties and structure morphology of fresh and spent samples. DRIFTS investigation confirmed the formation of mono- and bidentate formates, CH_2O, and CH_3O intermediate species suggesting that the reaction mechanism follows formate pathway for the synthesis of methanol from CO_2 hydrogenation over CaPdZn/CeO_2.

Key words: CO_2 hydrogenation, methanol, CaPdZn/CeO_2 catalyst, DRIFTS, reaction mechanism.

INTRODUCTION

Carbon dioxide utilisation as a feedstock for industrial production of valuable chemicals has recently been involved as an active area of catalysis research. The utilisation of CO_2 was addressing the possible solution of critical issues like global warming, depleting of high quality fossil fuel sources, and availability of a cheap and abundant CO_2 raw material for the synthesis of different chemical products [1,2]. Carbon dioxide hydrogenation to methanol is the most viable route for application of the former. Methanol serves as an excellent energy storage material alternative to traditional fossil fuels as well as a fuel for direct methanol fuel cell [3–5].

Palladium-based catalysts have exhibited superior catalytic performance in recent years, especially in the reaction of methanol synthesis from CO_2 and H_2 [6–9]. The properties of these catalysts are strongly influenced by preparation method [10–12] and catalyst reduction procedure [7,8,12,13] as well as by type of support [14–17] and promoter [18,19]. Synergic effects and chemistry of the strong metal support and metal-metal interaction of Pd and ZnO have also been widely studied. Pd/ZnO system appeared to be highly active towards methanol formation from CO_2 [6–9,12,14,20]. The observed high catalytic activity of this system is associated mainly with the formation of PdZn bimetallic alloy, which was formed due to electrons transfer from Pd to ZnO at elevated temperatures over 500 °C of catalyst reduction [6–9,12].

In the present study, we report results of DRIFTS study of methanol synthesis from CO_2 and H_2 on CaPdZn/CeO_2 catalyst. A reaction mechanism was proposed based on evidences obtained from spectroscopic registration of the formation of various intermediate species over the catalyst surface during the reaction of methanol synthesis from CO_2 and H_2.

The catalyst was prepared by the chelating method employing citric acid as a chelating agent. This method was previously used for synthesising nanosized high surface area CeO_2 particles. The citric acid was used as a chelating agent for its well-known positive contribution in controlling the morphology of the metal particles size and useful assistance to avoid sintering of synthesized nanomaterials [21–23].

EXPERIMENTAL

Catalyst preparation

A typical preparation procedure of 2.0 g of CaPdZn/CeO_2 sample is presented in the following lines.

Needed amounts of desired catalyst component salts were dissolved in separate beakers containing 30 cm^3 deionised water, i.e. 0.2165 g of Pd (palladium(II) nitrate hydrate ≥99.9%-metal basis, Alfa Aesar), 0.4549 g of Zn (zinc nitrate hexahydrate ≥98%, Aldrich Chemical Company), 0.059 g of Ca (calcium nitrate tetrahydrate, Techno Pharmchem

* To whom all correspondence should be sent
E-mail: zfsharif@gmail.com; sfzaman@kau.edu.sa

≥99.0%), and 4.516 g of Ce (cerium(III) nitrate hexahydrate ≥99.0%, Fluka Analytical).

An aqueous solution of 8.2702 g citric acid (≥99%, Techno Pharmchem, India) at a 1:3 molar ratio of metal ion (Pd, Zn, Ca and Ce) present in a particular catalyst sample to citric acid, was added dropwise into Ce salt solution and heated at 50 °C for 15 min under continuous stirring. Later, Pd, Zn, and Ca salt solutions were added dropwise into the mixture of Ce salt and citric acid and heated at 90 °C for 6 h until a brownish yellow gel-like mixture was formed. The resulting mixed gel was aged for 24 h at 90 °C in a water bath and later placed into an oven for 18 h at 110 °C resulting in a completely dried solid residue. Afterwards, it was crushed into powder and calcined in dry air at 300 °C for 2 h and then at 500 °C for 3 h.

Catalyst characterisation

BET surface area and pore size distribution were analysed by N_2 adsorption-desorption method at liquid nitrogen temperature with N_2 as adsorbate. NOVA 2200e (Surface area & Pore size Analyzer, Quantachrome Instruments) apparatus was used. Before each analysis, samples were dried at 300 °C for 2 h under vacuum.

X-ray diffraction patterns were collected in order to identify the crystal phases contained in the calcined, passivated, and spent samples. An Equinox 1000 (Inel, France) XRD equipment (Co Kα = 1.789 Å X-ray source and generator settings: 30 kV, 30 mA) with the real-time acquisition in 2θ range of 0–110° for 7200 s were used for these measurements.

H_2-TPR experiments were conducted to study the reduction behaviour of the calcined catalysts using Pulsar automated chemisorption analyser (Quantachrome Instruments). In general, 0.1 g of sample was loaded into U-type quartz reactor. Then the temperature was raised and maintained at 120 °C under helium flow for 1 h to remove any entrapped moisture. After cooling the sample back to 40 °C, a 5% H_2 in N_2 mixture was introduced at 15 cm^3min^{-1} and the temperature was linearly raised to 800 °C at a 5 °Cmin^{-1} ramping rate. A TCD detector was used to analyse the effluent stream.

CO_2-TPD measurements were employed to examine catalyst sample basicity using Pulsar automated chemisorption analyser (Quantachrome Instruments). Prior to CO_2 adsorption, catalyst samples (0.1 g each) were first reduced at 550 °C under H_2 flow (20 cm^3min^{-1}) for 1 h and then brought to room temperature under He flushing (15 cm^3min^{-1}) for 2 h. The reduced samples were then saturated with 15% CO_2/N_2 mixture (20 cm^3min^{-1}) for 1 h. Afterwards, TPD analysis was prompted at a heating rate of 10 °C/min under He flow (15 $cm^3min^{-1}n$) and desorbed amount of CO_2 was detected by a mass spectrometer. The amount of desorbed CO_2 was calculated by comparing the integrated peak area of CO_2-TPD curve to the area of the CO_2 calibration pulse.

In order to understand and identify the intermediate species and general reaction mechanism, in situ IR spectra were recorded on a Tensor II FTIR spectrometer (Bruker) installed with DRIFT accessories, Harrick praying mantis, and zinc selenide window capable of achieving pressure up to 40 bar. In general, 0.1 g of calcined sample was placed in the IR cell and reduced at 550 °C under H_2 flow (20 cm^3min^{-1}) for 1 h. Subsequently, the temperature was lowered back to 230 °C under Ar flow (15 $mlmin^{-1}$) and a background IR spectrum was recorded after 3 h of Ar flushing of the reaction chamber at reaction temperature. Then, CO_2 and H_2 mixture flow (20 cm^3min^{-1}) was introduced with an applied pressure of 30 bar. Totally 91 DRIFT spectra were collected for 3 h at 2 min time interval. Each spectrum was an average of 100 scans at 4 cm^{-1} resolution.

To investigate the catalyst structure and morphology at nanoscale, HRTEM and EDX analyses of freshly reduced $CaPdZn/CeO_2$ catalyst were also performed employing a 200 kV D1234 Super Twin microscope (Technai, Netherlands).

Catalytic activity tests

Activity tests of $CaPdZn/CeO_2$ catalysts were carried out in a MA-Effi reactor (PID Eng & Tech, Spain) equipped with Bronkhorst mass flow controllers and temperature sensors and controllers. A reaction mixture at a flow rate of 20 cm^3min^{-1} and pressure of 30 bar and composition of CO_2:H_2 = 1:3 was used. The reactor was charged with 0.5 g of catalyst. Prior to each test, the sample was reduced *in situ* at 550 °C with 20 cm^3min^{-1} H_2 gas flow for one hour at atmospheric pressure.

The reaction products were analysed using an Agilent 7890 A gas chromatograph equipped with a TCD detector with HayeSep Q packed column for CO_2, CO, and CH_4 analysis and a FID detector with HP-Pona capillary column (19091S-001E) for methanol and higher hydrocarbons analysis. Reported data on conversion and selectivity were obtained by an average of three independent readings with an error range of ±3% taken after 3 h of reaction run. CO_2 conversion and selectivity of products were defined as follows:

$$CO_2 conv = \frac{(\text{Moles } CO_{2\,in} - \text{Moles } CO_{2\,out}) \times 100}{\text{Moles } CO_{2\,out}}, \% \quad (1)$$

$$CH_3OH \text{ sel} = \frac{\text{Moles } CH_3OH \times 100}{\text{Moles } (CH_3OH + CO + CH_4) \text{ in product stream}}, \% \quad (2)$$

RESULTS AND DISCUSSION

Structural properties and catalytic performance

Figure 1 shows XRD profiles of calcined and reduced $CaPdZn/CeO_2$ samples. Diffraction peaks for CeO_2 phase [PDF 00-034-0394] were observed at 2θ= 33.28, 38.61, 55.74, 66.48, 69.86, 82.77, 92.19, 95.32, 108.13, 118.38, 138.48, 155.87, and 165.31° for calcined and reduced $CaPdZn/CeO_2$ sample. For reduced $CaPdZn/CeO_2$ sample, intense peaks at 2θ = 48.19 and 51.74° were detected reflecting the presence of PdZn alloy phase with (111) and (200) crystal planes [PDF 03-065-9523]. This confirms the formation PdZn alloy phase as shown in figure 1. At a higher reduction temperature (>500 °C), metal-to-metal interaction causes the transfer of electrons between metallic palladium and ZnO, hence forming the PdZn-bimetallic alloy. Several previous studies asserted that PdZn alloy phase served as the catalytically active phase for con-verting CO_2 to methanol [6–8, 20].

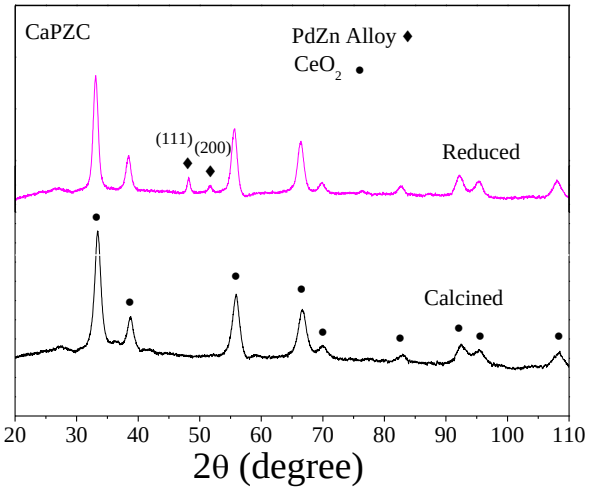

Fig. 1. XRD profile of calcined and reduced $CaPdZn/CeO_2$ catalyst.

Table 1 lists the physiochemical data and catalytic performance of ceria carrier and $CaPdZn/CeO_2$ catalyst. Catalyst surface area was 67 m^2g^{-1}, being much higher compared to the support CeO_2 which had a surface area of 52 m^2g^{-1}.

Table 1. Textural and catalytic properties of the $CaPdZn/CeO_2$ and CeO_2

Catalyst	Surface area S_{BET} m^2/g	Pd Dispersion %	Desorbed CO_2 $\mu mole/g_{cat}$	CO_2 conversion %	CH_3OH Selectivity %
$CaPdZn/CeO_2$	67	7.6	88.0	7.7	100.0
CeO_2	52	-	42.0	-	-

The increase of surface area with the insertion of various metals over CeO_2 support might be attributed to the chelating preparation procedure. Basicity of the $CaPdZn/CeO_2$ sample was also enhanced as the desorbed amount of CO_2 from the catalyst (88 $\mu molg_{cat}^{-1}$) was much larger than the amount of CO_2 desorbed from catalyst support, CeO_2 (42 $\mu molg_{cat}^{-1}$).

Figure 2 displays a HRTEM image of reduced $CaPdZn/CeO_2$ sample. PdZn alloy particles, formed at high temperature reduction, were well dispersed and uniformly distributed over CeO_2 support which was confirmed by HRTEM. Figure 3 illustrates the EDS image of reduced $CaPdZn/CeO_2$ catalyst enlisting elemental composition of Pd, Ce, Zn, and Ca, which agrees with the amounts used for catalyst synthesis.

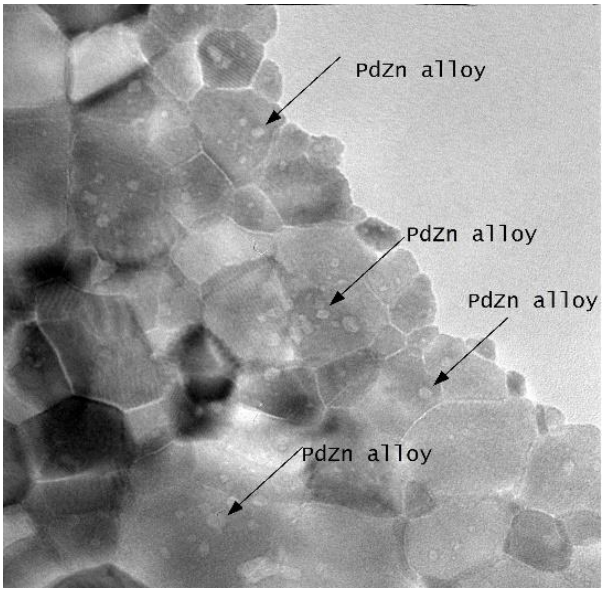

Fig. 2. HRTEM image of reduced $CaPdZn/CeO_2$ catalyst.

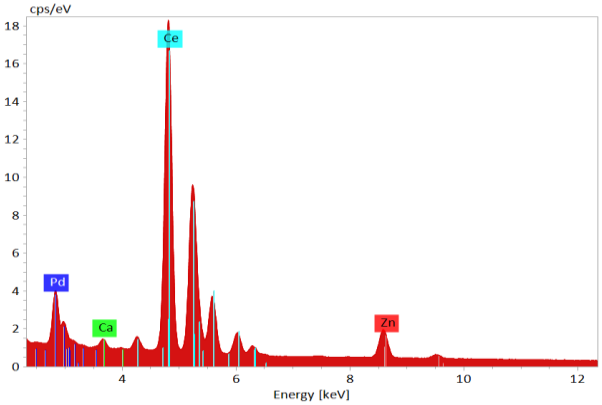

Fig. 3. EDS of reduced $CaPdZn/CeO_2$ catalyst. (Bruker Quantax XFalsh 6 solid angle of a 30-mm^2 active area chip energy resolution 123 eV at Mn Kα, 45 eV at C).

Catalytic activity testing

The catalytic activity of $CaPdZn/CeO_2$ samples was tested at different temperatures in the range of 220–270 °C and pressure of 30 bar. The conversion of CO_2 was improved appreciably with the increase of temperature but methanol selectivity was decreased as presented in Table 2. Methanol selectivity decrease may have occurred mainly due to reverse water-gas shift (RWGS) reaction, forming CO as a by-product at elevated temperatures above 220 °C. Generally, at higher temperatures, RWGS reaction (Eqn. 3) dominates and hinders methanol formation due to thermodynamic constrains [21].

$$CO_{2(g)} + H_{2(g)} \leftrightarrow CO_{(g)} + H_2O_{(g)};\ \Delta H_{298\,K} = 41\ \text{kJ/mol} \quad (3)$$

Table 2. Catalytic activity of $CaPdZn/CeO_2$ catalyst

	220 °C	230 °C	250 °C	270 °C
Conversion (%X)	7.7	8.3	10.8	11.25
Methanol selectivity (%S)	~100	97.4	90.0	78.0

(Reaction conditions: Catalyst weight = 0.5 g; Pressure = 30 bar, reaction mixture composition H_2:CO_2 = 3:1, flow rate = 20 cm^3min^{-1}. Reduction temperature 550 °C)

In situ DRIFTS analysis

We have selected the temperature of 230 °C for DRIFT mechanistic study as at this point, we have observed moderate CO_2 conversion and high methanol (>97%) selectivity. *In situ* DRIFTS analysis was carried out to evaluate the emergence of various intermediate species formed over the catalyst surface with time at 230 °C and pressure of 30 bar for CO_2 hydrogenation to methanol. DRIFTS results assisted in developing a perception of the actual reaction sequence occurred over the surface of the tested catalyst and helped to distinguish the surface species relevant to the mechanism of selective formation of methanol.

DRIFT spectra, which were registered for reaction time of 180 minutes at interval of 5 minutes, exhibited unique characteristics of emerging intermediate surface species as presented in figure 4. Surface concentrations of the intermediate species were gradually increased at the beginning of the reaction and reached a maximum for 90 minutes after introduction of the reaction mixture to the DRIFT chamber. The DRIFT spectral range of acquisition was divided into five regions (R1-R5 as shown in figure 4) based on the unique band characteristics of various detected surface species. Figure 5 shows an enlarged image of IR spectral acquisition at different time intervals with the evolution of different surface species. Carbonates (bridged, monodentate and bidentate) and inorganic carboxylate species, which usually appear at low temperature CO_2 adsorption on ceria [24], could not be observed as they normally were converted to corresponding formate species at temperature above 200 °C in a very short time [25].

At the beginning of the registration of IR spectra, no characteristic bands due to the presence of formates were registered. After 5 min onward, IR bands appeared at 1640, 1575, and 1340 cm^{-1} (Region R2) indicating the emergence of monodentate (m-HCOO) and bidentate (b-HCOO) formate species [26–28] attributed to hydrogenation of carbonaceous species at elevated temperature. IR bands at 1746 and 2843 cm^{-1} corresponded CO-stretching vibrations (Region R3) and CH_2-stretching vibration ascribed to gas phase CH_2O species. IR bands at 2831, 2942, and 3077 cm^{-1} (Region R5) may be assigned to methoxy (CH_3O) species [26,29,30], which was evolved by stepwise hydrogenation of formate and CH_2O species. A strong feature for CO_2 (gas phase non-dissociative adsorption over CeO_2 surface) can also be observed between 2250 and 2400 cm^{-1} (Region R4). Band intensity in this region was consistent throughout the reaction time showing a strong interaction of CeO_2 with acidic CO_2. IR bands appearing at 2090 and 2177 cm^{-1} (Region R3) may be attributed to linearly adsorbed CO (CO_L) on Ce^{+4} [24] and gas phase CO, respectively, due to the adsorption of CO_2 on oxygen vacancies over the surface of ceria support. Formation of gaseous methanol was also evident (almost after 5 min of introducing reaction mixture at reaction conditions) from the bands arisen at 1005, 1031, and 1055 cm^{-1} (gaseous methanol) and 2844 cm^{-1} (gas phase CH_3 *s*-stretching), and 3000 cm^{-1} (gas phase CH_3 *d*-stretching) corresponding to methanol formation.

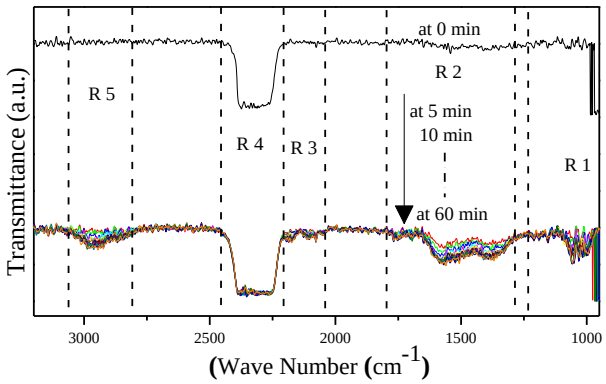

Fig. 4. DRIFT spectral acquisition at different time intervals of reduced $CaPdZn/CeO_2$ catalysts at 230 °C and 30 bar.

Figure 5 presents the appearance of gaseous CH_3OH species with time during the CO_2 hydrogenation reaction. The band at 1055 cm^{-1} was used to analyse the dynamics of CH_3OH rise with time

(Fig. 6). It has been reported that PdZn alloy formation assists the selective formation of methanol [7,8]. It is well known that the type of preparation method, used support, and promoters may influence strongly the catalytic performance of the catalyst. Metal-support interaction also enhances the catalytic performance in the case of supported Pd catalysts and this phenomenon was also observed in our CaPdZn/CeO_2 catalyst [6,9]. It may be assumed that the adsorption ability of CO_2 and oxygen-containing intermediate species (such as OH^-, HCO^-, H_2CO, H_2COO, HCOO, and H_3CO) is higher at CaPdZn/CeO_2 interface. A density functional study is required to prove this claim though.

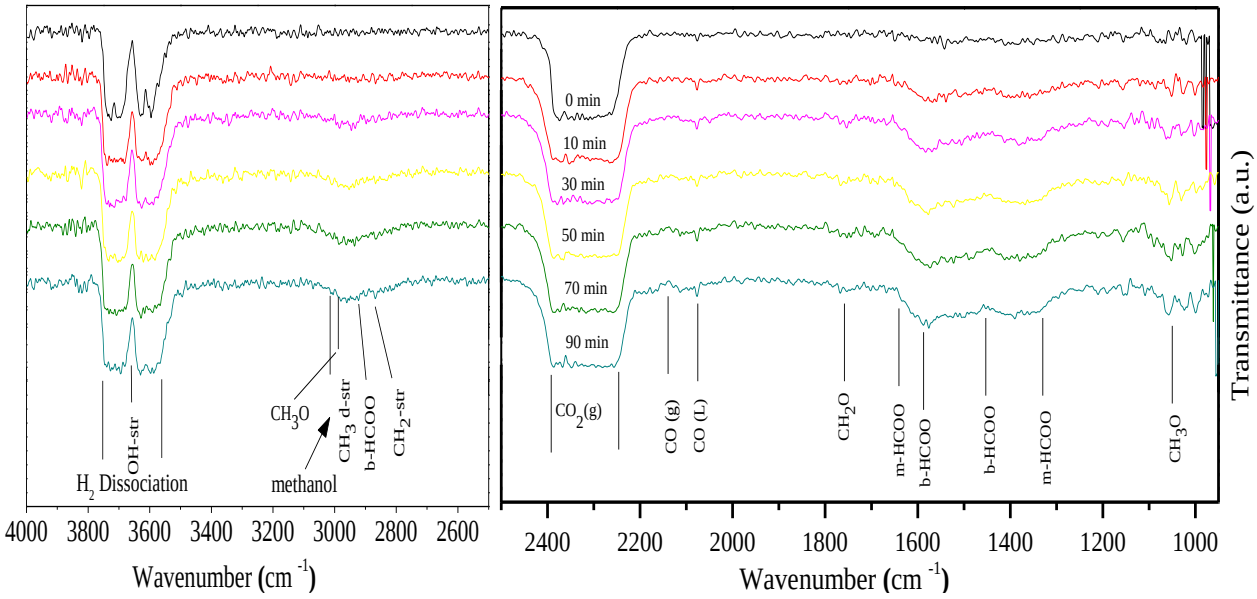

Fig. 5. Identification of various surface species for methanol synthesis from CO_2 using CaPdZn/CeO_2 catalysts at 230 °C and 30 bar pressure.

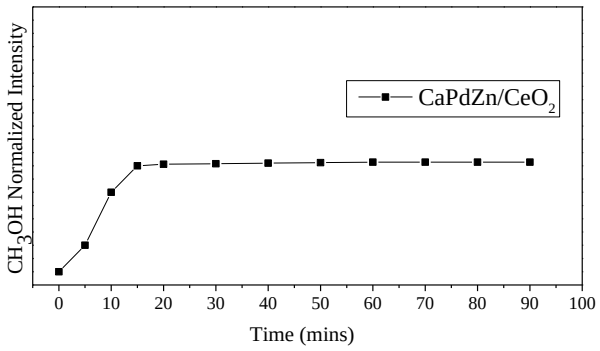

Fig. 6. Band intensity of gaseous methanol in the reaction products as a function of reaction time over CaPdZn/CeO_2 catalyst.

Reaction mechanism

In situ DRIFT study provided the necessary evidence required to propose a general reaction mechanism of CH_3OH formation over CaPdZn/CeO_2 catalyst. Formation of m-HCOO, b-HCOO, CH_2O, and CH_3O were kinetically favourable over the catalyst surface. Furthermore, no clear evidence of COOH species formation was observed indicating that the CaPdZn/CeO_2 system inhibits the RWGS reaction and leads the reaction sequence to follow the formate pathway. Dissociative adsorption of hydrogen on PdZn alloy generated activated H adatoms, which ultimately lowered the reaction energy barrier for HCOO pathway. A strong metal support interaction (SMSI) between PdZn bimetallic alloy and CeO_2 allowed activation of CO_2 over the catalyst surface and facilitated spillover of H adatoms onto the support thereby increasing the hydrogenation rate of adsorbed carbonaceous species. These results were in line with previous reports on Pd-based systems for CO_2 hydrogenation [25,31,32]. Based on our findings, we may suggest a dual-site (bifunctional) reaction mechanism for CO_2 hydrogenation over CaPdZn/CeO_2 yielding CH_3OH and CO only as also discussed elsewhere [25,31,33]. Adsorbed carbonaceous species (monodentate, bidentate, and polydentate carbonate, etc.) over CeO_2 were stepwise hydrogenated to formates (m-HCOO and b-HCOO) with the supply of H adatoms from the dissociation of H_2 on PdZn alloy. This formate species was further hydrogenated to CH_2O, methoxy CH_3O species, and finally to methanol and CO. A general reaction mechanism is illustrated in Scheme 1.

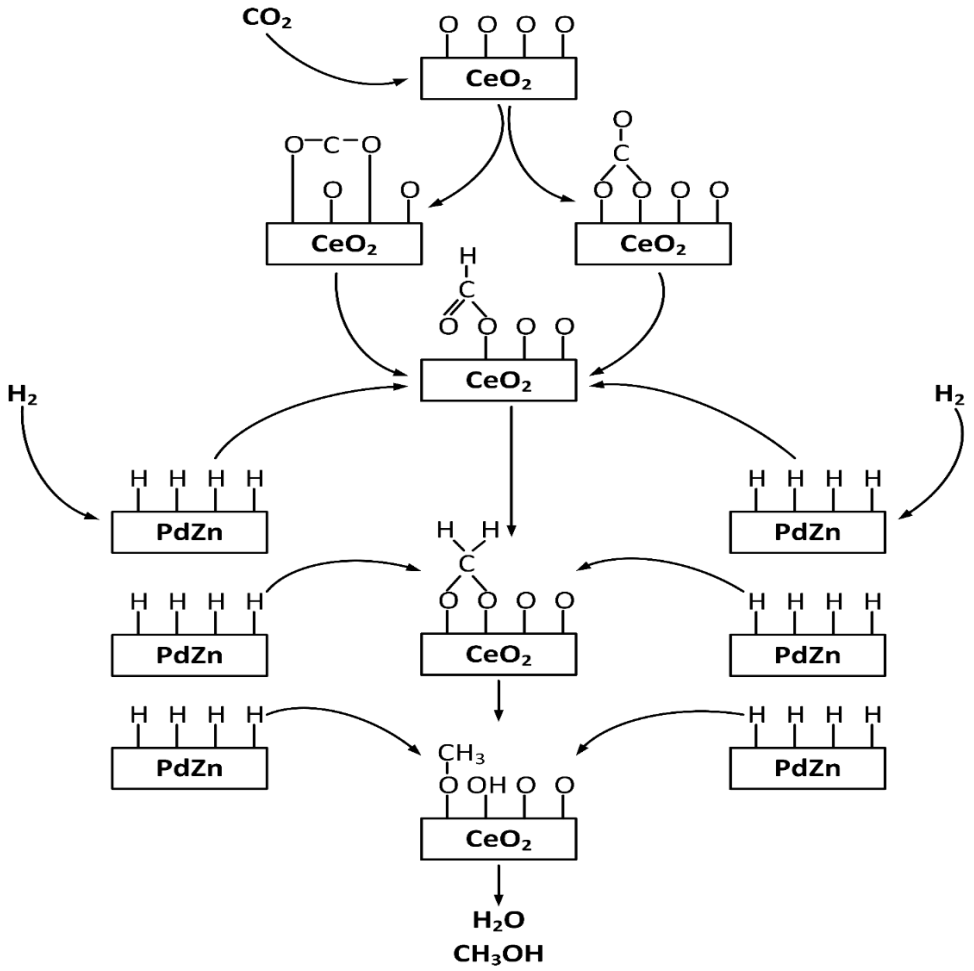

Scheme 1. Proposed reaction mechanism based on *in situ* DRIFTS data on methanol synthesis from CO_2 and H_2 over CaPdZn/CeO_2 catalyst.

CONCLUSIONS

The CaPdZn/CeO_2 catalyst exhibits ~100% selectivity to methanol and 7.7% of CO_2 conversion at low temperature of 220 °C and pressure of 30 bar. The reason for this excellent selectivity and activity lies in the strong H_2 dissociation ability of PdZn alloy to actively hydrogenate the adsorbed carbonaceous species as well as the strong adsorption of CO_2 over CeO_2 support as it provides a platform and stability to carbonaceous species formed over the catalysts surface. *In situ* DRIFT analysis confirmed the formation of formate species and its subsequent conversion to methoxy species, and then finally to methanol, suggesting a formate pathway for methanol synthesis from CO_2 hydrogenation using CaPdZn/CeO_2 under tested reaction conditions.

Acknowledgment: *The support of Deanship of Graduate Studies at King Abdulaziz University for the Postgraduate Scholarship for International students is highly appreciated.*

REFERENCES

1. F. T. Zangeneh, S. Sahebdelfar, M. T. Ravanchi, *J. Nat. Gas Chem.*, **20**, 219 (2011).
2. G. A. Olah, *Catal. Lett.*, **93**, 1 (2004).
3. F. Pontzen, W. Liebner, V. Gronemann, M. Rothaemel, B. Ahlers, *Catal. Today*, **171**, 242 (2011).
4. F. Liao, Z. Zeng, C. Eley, Q. Lu, X. Hong, S. C. E. Tsang, *Angew. Chem. Int. Ed.*, **51**, 5832 (2012).
5. J. Nakamura, T. Uchijima, Y. Kanai, T. Fujitani, *Catal. Today*, **28**, 223 (1996).
6. H. Bahruji, M. Bowker, J. Hayward, G. Hutchings, W. Jones, J. R. Esquius, *Farad. Disc.*, **197**, 309 (2017).
7. H. Bahruji, M. Bowker, G. Hutchings, N. Dimitratos, P. Wells, E. Gibson, W. Jones, C. Brookes, D. Morgan, G. Lalev, *J. Cat.*, **343**, 133 (2016).
8. X.-L. Liang, X. Dong, G.-D. Lin, H.-B. Zhang, *Appl. Catal. B: Environ.*, **88**, 315 (2009).
9. J. Xu, X. Su, X. Liu, X. Pan, G. Pei, Y. Huang, X. Wang, T. Zhang, H. Geng, *Appl. Catal. A: Gen.*, **514**, 51 (2016).
10. L. Fan, K. Fujimoto, *J. Catal.*, **150**, 217 (1994).
11. L. Fan, K. Fujimoto, *J. Catal.*, **172**, 238 (1997).

12. C.-H. Kim, J. S. Lee, D. Trimm, *Top. Catal.*, **22**, 319 (2003).
13. L. Fan, K. Fujimoto, *Appl. Catal. A: Gen.*, **106**, L1 (1993).
14. Y. A. Ryndin, R. Hicks, A. Bell, Y. I. Yermakov, *J. Catal*., **70**, 287 (1981).
15. T. Fujitani, M. Saito, Y. Kanai, T. Watanabe, J. Nakamura, T. Uchijima, *Appl. Catal. A: Gen.*, **125**, L199 (1995).
16. W.-J. Shen, M. Okumura, Y. Matsumura, M. Haruta, *Appl. Catal. A: Gen*., **213**, 225 (2001).
17. P. J. Berlowitz, D. W. Goodman, *J. Catal*., **108**, 364 (1987).
18. J. Driessen, E. Poels, J. Hindermann, V. Ponec, *J. Catal*., **82**, 26 (1983).
19. V. Ponec, *Surf. Sci*., **272**, 111 (1992).
20. N. Iwasa, H. Suzuki, M. Terashita, M. Arai, N. Takezawa, *Catal. Lett*., **96**, 75 (2004).
21. J. Trujillo-Reyes, A. Vilchis-Nestor, S. Majumdar, J. Peralta-Videa, J. Gardea-Torresdey, *J. Haz. Mat*., **263**, 677 (2013).
22. T. Masui, H. Hirai, N. Imanaka, G. Adachi, T. Sakata, H. Mori, *J. Mat. Sci. Lett*., **21**, 489 (2002).
23. C. H. Wang, S. S. Lin, *Appl. Catal. A: Gen*., **268**, 227 (2004).
24. C. Li, Y. Sakata, T. Arai, K. Domen, K.-I. Maruya, T. Onishi, *J. Chem. Soc. Faraday Trans. 1*, **85**, 929 (1989).
25. S. E. Collins, M. A. Baltanás, A. L. Bonivardi, *J. Catal*., **226**, 410 (2004).
26. G. C. Cabilla, A. L. Bonivardi, M. A. Baltanás, *J. Catal*., **210**, 213 (2001).
27. D. H. Gibson, *Coord. Chem. Rev*., **185**, 335 (1999).
28. R. Burch, S. Chalker, J. Pritchard, *J. Chem. Soc*., *Faraday Trans*., **87**, 193 (1991).
29. J. Weigel, R. Koeppel, A. Baiker, A. Wokaun, *Langmuir*, **12**, 5319 (1996).
30. L. J. Burcham, L. E. Briand, I. E. Wachs, *Langmuir*, **17**, 6164 (2001).
31. S. E. Collins, J. J. Delgado, C. Mira, J. J. Calvino, S. Bernal, D. L. Chiavassa, M. A. Baltanás, A. L. Bonivardi, *J. Catal*., **292**, 90 (2012).
32. N. Rui, Z. Wang, K. Sun, J. Ye, Q. Ge, C.-J. Liu, *Appl. Catal. B: Environ.*, **218**, 488 (2017).
33. X. Guo, D. Mao, G. Lu, S. Wang, G. Wu, *J. Mol. Cat. A: Chem.*, **345**, 60 (2011)...

ИЗСЛЕДВАНЕ С ДОИЧС НА МЕХАНИЗМА НА СИНТЕЗ НА МЕТАНОЛ ОТ CO_2 И ВОДОРОД С КАТАЛИЗАТОР $CaPdZn/CeO_2$

А. С. Малик*, Ш. Ф. Заман[1], А. А. Ал-Захрани, М. А. Даус, Х. Идрис, Л. А. Петров

Департамент по инженерна химия и материалознание, Инженерен факултет, Университет „Крал Абдулазис“, п.к. 80204, 21589 Джеда, Саудитска Арабия

Постъпила на 2 февруари 2018 г.; Преработена на 23 март 2018 г.

(Резюме)

В настоящата работа са представени резултати от DRIFTS изследване на механизма на синтез на метанол от CO_2 и H_2 върху катализатор $CaPdZn/CeO_2$. Катализаторът притежава превъзходни каталитични свойства. Селективността на процеса при 220 °C и налягане 30 атм. е 100% при 7.7% конверсия на CO_2. Измерванията с DRIFTS са проведени *in situ* при налягане 30 атм. и са проследени във времето промените в концентрациите на повърхностните междинни съединения. Катализаторът и използваният носител са охарактеризирани с метода БЕТ, хемосорбция на CO, ТПД на CO_2, рентгеноструктурен анализ и ТЕМ с висока разделителна способност. Установено е формирането на моно- и бидентантни формиати, CH_2O и CH_3O, което сочи че синтеза на метанол протича през формирането на формиати. Предложен е и вероятен механизъм на процеса на синтез на метанол от CO_2 и водород.